Movement Responses of Caribou to Human-Induced Habitat Edges Lead to Their Aggregation near Anthropogenic Features

Daniel Fortin,[1,*] Pietro-Luciano Buono,[2] André Fortin,[3] Nicolas Courbin,[1] Christian Tye Gingras,[3] Paul R. Moorcroft,[4] Réhaume Courtois,[5] and Claude Dussault[6]

1. Chaire de Recherche Industrielle, Conseil de recherches en sciences naturelles et en génie du Canada (CRSNG)–Université Laval en Sylviculture et Faune, Département de Biologie, Université Laval, Québec, Québec G1V 0A6 Canada; 2. Faculty of Science, University of Ontario Institute of Technology, 2000 Simcoe Street North, Oshawa, Ontario L1H 7K4, Canada; 3. Groupe Interdisciplinaire de Recherche en Éléments Finis, Chaire de Recherche Industrielle du CRSNG en calcul scientifique, Département de Mathématiques et de Statistique, Université Laval, Québec, Québec G1V 0A6 Canada; 4. Department of Organismic and Evolutionary Biology, Harvard University, Cambridge, Massachusetts 02138; 5. Service de la biodiversité et des maladies de la faune, Ministère des Ressources naturelles et de la faune, 880 chemin Sainte-Foy, Québec, Québec G1S 4X4 Canada; 6. Direction de l'expertise, Ministère des Ressources naturelles et de la faune, 3950 boulevard Harvey, 4e étage, Saguenay, Québec G7X 8L6 Canada

Submitted March 12, 2012; Accepted February 11, 2013; Electronically published April 12, 2013

Online enhancement: appendixes. *Dryad data:* http://dx.doi.org/10.5061/dryad.kh356.

ABSTRACT: The assessment of disturbance effects on wildlife and resulting mitigation efforts are founded on edge-effect theory. According to the classical view, the abundance of animals affected by human disturbance should increase monotonically with distance from disturbed areas to reach a maximum at remote locations. Here we show that distance-dependent movement taxis can skew abundance distributions toward disturbed areas. We develop an advection-diffusion model based on basic movement behavior commonly observed in animal populations and parameterize the model from observations on radio-collared caribou in a boreal ecosystem. The model predicts maximum abundance at 3.7 km from cutovers and roads. Consistently, aerial surveys conducted over 161,920 km^2 showed that the relative probability of caribou occurrence displays nonmonotonic changes with the distance to anthropogenic features, with a peak occurring at 4.5 km away from these features. This aggregation near disturbed areas thus provides the predators of this top-down-controlled, threatened herbivore species with specific locations to concentrate their search. The edge-effect theory developed here thus predicts that human activities should alter animal distribution and food web properties differently than anticipated from the current paradigm. Consideration of such nonmonotonic response to habitat edges may become essential to successful wildlife conservation.

Keywords: advection-diffusion model, animal movement, edge effects, human disturbance, woodland caribou.

* Corresponding author; e-mail: daniel.fortin@bio.ulaval.ca.

Am. Nat. 2013. Vol. 181, pp. 827–836.
0003-0147/2013/18106-53711$15.00.
DOI: 10.1086/670243

Introduction

Worldwide, conservation and management actions rely on an accurate assessment of anthropogenic disturbance effects. Landscapes are becoming increasingly fragmented by human activities (Watts et al. 2007), and significant effort has been devoted to understanding the resulting edge effects. A broad range of edge effects have been reported, with differences related to whether species benefit from the habitat occurring directly at the edge or whether they do not react to the edge per se but respond negatively or positively to the disturbance (Forman and Alexander 1998; Baker et al. 2002; Ries and Sisk 2004; Ries et al. 2004; Ewers and Didham 2007; Ewers et al. 2007; Girvetz et al. 2007; Eigenbrod et al. 2009; Wimp et al. 2011). Species responding negatively to human-induced habitat edges are of particular concern for the preservation of local populations. According to the prevailing edge-effect theories (Forman and Alexander 1998; Baker et al. 2002; Ries and Sisk 2004; Ries et al. 2004; Ewers and Didham 2007; Ewers et al. 2007; Girvetz et al. 2007; Eigenbrod et al. 2009; Wimp et al. 2011), the abundance of animals affected by human disturbance should increase monotonically as a function of distance from the edge, eventually reaching a plateau. Maximum densities should therefore occur farthest from the disturbance edge.

The behavioral mechanisms generating edge effects are poorly understood (Reeve and Cronin 2010). Nonetheless, the current paradigm has a strong influence on the design of empirical studies and the search for ecological patterns and, therefore, on our general understanding of edge ef-

fects. For example, edge-effect studies commonly restrict their evaluation to the functional form dictated by the prevailing theories (Ries and Sisk 2004; Ries et al. 2004; Ewers and Didham 2007). For a number of species, however, the relative probability of occurrence (which can translate into relative abundance; Boyce and McDonald 1999) increases up to a certain distance from human development before decreasing farther away (Boyce and Waller 2003; Johnson et al. 2005). These studies considered this apparent decrease after a threshold distance from human-induced habitat edges to be a methodological artifact caused by the failure to saturate the study area with collared animals, a supposition that can have consequences in conservation planning. For example, the future distribution of grizzly bears (*Ursus arctos*) in areas from which they had been extirpated was inferred by assuming an asymptotic edge-effect function scaled to saturate near the observed maximum, as proposed by the classical paradigm but unlike the pattern emerging from the actual analysis (Boyce and Waller 2003). Here, we propose a theoretical explanation for these observed patterns that is based on behavioral mechanisms.

Animals often adjust their movement to habitat edges, generally with directional biases varying with distance from stimulus sources (Schultz and Crone 2001; Moorcroft and Lewis 2006). Such distance-dependent taxis can result in animal aggregations adjacent to disturbed areas. Following habitat disturbance, for example, some animals leave disturbed sites to join neighbors located farther away, thereby creating an aggregation of conspecifics. This pattern can be reinforced by directional movement biases near the disturbance's edge, yielding asymmetrical boundary behavior with individuals being more likely to leave than to enter disturbed areas. Further, individuals often redistribute themselves over rather limited distances because of the high costs of moving to new and remote locations (Sutherland et al. 2000). This limit can result in highest animal abundances occurring in the vicinity of disturbed sites because of disturbance avoidance. Such a counterintuitive distribution pattern is not predicted by most prevailing theories (Forman and Alexander 1998; Baker et al. 2002; Ries and Sisk 2004; Ries et al. 2004; Ewers and Didham 2007; Ewers et al. 2007; Girvetz et al. 2007; Eigenbrod et al. 2009), but it can have far-reaching ecological consequences.

We formulated these ideas using an advection-diffusion partial differential equation (PDE) model reflecting multiscale movement decisions of forest-dwelling woodland caribou (*Rangifer tarandus caribou*) in managed forests. This ecotype of woodland caribou is endangered in Canada (Thomas and Gray 2002), and the decline of its populations and the recession of its range have been linked to logging activities (Courtois et al. 2003*b*, 2007; Schaefer 2003). The development of the forestry road network increases the accessibility of caribou habitat to humans, including aboriginal hunters and poachers (Courtois et al. 2003*b*, 2007; Schaefer 2003), as well as to wolves (*Canis lupus*), an important predator that often travels on roads (Ciucci et al. 2003; Courbin et al. 2009; Houle et al. 2010; Whittington et al. 2011). Also, logging brings harvested stands back to an early seral stages, thereby increasing the habitat quality of the black bear (*Ursus americanus*; Brodeur et al. 2008). This opportunistic predator (Bastille-Rousseau et al. 2011) can have a strong impact on juvenile recruitment of caribou populations (Pinard et al. 2012). Moose (*Alces alces*) also benefit from logging, because deciduous vegetation begins to invade the harvested stands. An increase in the moose population can result in higher wolf density, which in turn can affect caribou populations. A common outcome of forest harvesting is therefore a higher mortality rate of caribou in areas where early seral stands make up a large proportion of the landscape (Courtois et al. 2007; Wittmer et al. 2007). The dynamics of caribou populations should depend strongly on the range and functional form of edge effects resulting from logging activities, but the underlying mechanisms of these effects remain poorly understood.

The PDE model was parameterized with two independent data sets of caribou locations. Animal distribution results from multilevel and multiscale decisions (e.g., Johnson 1980; Bailey et al. 1996; Boyce 2006; Moreau et al. 2012); accordingly, our model integrates observations gathered at different scales to predict the distribution of caribou as a function of their responses to anthropogenic disturbances. At the finest scale, we quantified directional biases in the movement of caribou within their home ranges. At a broader scale, we determined whether caribou shift their activity centers from one year to the next following the expansion of the road network and logged areas. After incorporating this information into the PDE model, we then tested the model's numerical solutions by using a third data set consisting of track surveys of caribou collected over 161,920 km^2 of boreal forest in winter. Given that track surveys of caribou were available only in winter, we restricted our entire study to that season.

Development of Movement Model

We used a Fokker-Planck equation (see Moorcroft and Lewis 2006) to describe the temporal changes in caribou distribution (on a given domain) as a probability density function. Similar models have been used previously in ecological modeling. Moorcroft et al. (2006), for example, developed a scent-mark boundary model for coyotes for which the advection term in the PDE depends on the density of scent marks associated with each pack. In our

case, the advection term relates to anthropogenic disturbances, and the model is designed to assess the impact of human-induced edge effects on caribou redistribution. Let $\nu(\mathbf{x}, t)$ be the probability of being at $\mathbf{x} = (x, y)$ in a domain Ω at time t, and consider that movement is driven by diffusion and is constrained by the distance to the nearest human-disturbed area and by home-range behavior. From probabilistic assumptions (see app. A, available online), we derive the following equation for the expected animal distribution:

$$\frac{\partial \nu(\mathbf{x}, t)}{\partial t} = \underbrace{\nabla \cdot \left(\frac{\rho_0^2}{2} \nabla \nu\right)}_{\text{Diffusion}} - \underbrace{\nabla \cdot \left(\frac{\rho_0^2}{2} b \mathbf{V}_\varepsilon(\mathbf{x}) \nu\right)}_{\text{Reaction to disturbance}}, \quad (1)$$

where ρ_0 is the mean move length, b is the bias per unit length traveled, and $\mathbf{V}_\varepsilon(\mathbf{x})$ is a continuous vector field describing the directed motion of the animal at **x.**

Two behaviors are encoded in the vector field $\mathbf{V}_\varepsilon(\mathbf{x})$: taxis in response to human disturbance for individuals located less than Δ from the disturbed areas and movement dominated by diffusion as the distance reaches and exceeds Δ. In other words, the magnitude and direction of the advection term reflect preferential movement by individuals as given by the vector field $\mathbf{V}_\varepsilon(\mathbf{x})$, which depends on the location of the nearest human-disturbed area. The parameter ε is the distance at which the repulsive effect of the edge of the disturbance vanishes, whereas Δ identifies the distance from the edge of the disturbance at which the boundary effect starts decaying to 0.

Accordingly, let $\mathbf{x}_b = (x_b, y_b)$ be a point on the edge of a human-disturbed area nearest to $\mathbf{x}$, and let $\mathbf{v}_b$ be the vector joining $\mathbf{x}$ to $\mathbf{x}_b$. Letting $\delta(\mathbf{x}) = \|\mathbf{x}_b - \mathbf{x}\|$, we derive $\mathbf{V}_\varepsilon(\mathbf{x}) = a_\varepsilon(\delta(\mathbf{x}))\mathbf{v}_b$, where a_ε is a continuous function defined as follows. For animals located in the vicinity of the disturbed area ($\delta(\mathbf{x}) < \Delta$), we set $a_\varepsilon(\delta(\mathbf{x})) = -1$ if $\mathbf{x}$ is in or at the edge of a disturbed region, with a_ε monotonically increasing such that $a_\varepsilon = 0$ if $\delta(\mathbf{x}) = \varepsilon$. For $\delta(\mathbf{x}) \geq \Delta$, $a_\varepsilon(\delta(\mathbf{x}))$ decreases exponentially to 0 from $a_\varepsilon(\Delta)$ (see app. A for details). The model is based on ρ_0 and b, and appendix A explains how we quantified these two parameters. The model requires the quantification of ε and Δ, which we do by using two independent data sets of locations of forest-dwelling caribou, as described in the next section. The numerical computations were performed using MEF++, finite-element-method research software created, developed, and maintained by the Groupe Interdisciplinaire de Recherche en Éléments Finis (GIREF) of the Université Laval in Québec, Canada (http://giref.ulaval.ca/mef.html; accessed September 4, 2012).

Methods

Model Parameterization

Our movement model was parameterized on the basis of the movements and spatial distribution of forest-dwelling caribou monitored with global-positioning-system (GPS) and very-high-frequency (VHF) collars in the Côte-Nord region of Québec, Canada. The Côte-Nord study area (51°00′N, 69°00′W) is characterized by a large proportion of old-growth conifer forest dominated by black spruce (*Picea mariana*), balsam fir (*Abies balsamea*), and jack pine (*Pinus banksiana*). Mean daily temperatures range from −23°C in January to 14°C in July, while mean annual precipitation is 715 mm (Crête and Courtois 1997). Forest harvesting has been the major source of anthropogenic disturbance for the past decade (Courtois et al. 2008).

Quantification of ε. We monitored 22 female caribou between 2005 and 2009, from December through April. Individuals were captured with a net gun fired from a helicopter and were fitted with GPS (Lotek Engineering, Newmarket, Ontario, Canada) or Argos/GPS (Telonics, Mesa, AZ) collars giving a GPS data set with 8-h interval locations. Each caribou was followed over 1.6 ± 0.2 winters (mean ± SE; range: 0.4–4 winters), with six individuals being followed during a single winter. We used the GPS data to determine whether caribou consistently alter the orientation of their movements with respect to the nearest clear-cut or road. Distance estimates came from a geographic information system in which the location of roads and cutblocks was updated every year on the basis of information from the local forestry companies. We found no overall directional bias based on the entire data set; however, the step-length distribution appeared to include a mixture of short and long steps. This heterogeneity could reflect the presence of multiple movement behaviors (Fryxell et al. 2008). We thus split the location data into camps (i.e., areas of home range that are used during an extended period of time, such as 1–4 weeks; Bailey et al. 1996), using the quantitative approach proposed by Barraquand and Benhamou (2008). The method is based on the clustering of local residency times, given the sequence of successive path locations. The circle's diameter averaged 2,254 ± 110 m and ranged between 800 and 3,000 m, depending on animal and year. GPS locations could be located outside the circle for no more than 48 h while still being part of the same residence-time event. After data clustering, we restricted our investigation to directional biases with respect to human disturbances during the intercamp moves of caribou that had traveled at least once within 10 km of a cut or a road ($n = 16$ individuals). We calculated the average vector direction of each caribou for every 1-km bin up to 9 km from the nearest road or cut,

for 2-km bins at distances of 9–15 km, and for a single bin at 16–20 km (fig. B1 in app. B, available online). A vector was estimated as long as the individual had made at least three intercamp moves in the distance category. Larger distance bins were necessary at greater distances to insure that we were able to estimate a minimum of one vector for every distance category. We then organized these average vectors along a linear scale ranging from −90° to +90°; these limits correspond, respectively, to a vector oriented perpendicularly away from the disturbance and a vector leading directly toward the disturbance. The vector direction of each bin was then related to the bin's mid-distance value using mixed-effects models with Gaussian distribution, with individuals being considered a random effect.

Recall that parameter ε in the vector field term $\mathbf{V}_{\varepsilon}(\mathbf{x})$ of the PDE model is the distance at which the repulsive effect of the edge of the disturbance vanishes. We estimate ε as the x-intercept of the regression curve (i.e., the 0° line), the distance where the statistical model predicts a movement perpendicular to cuts or roads.

To provide a general characterization of home-range size and composition, we used a 100% Brownian bridge kernel (Horne et al. 2007) to delineate the home ranges of GPS-collared individuals. We considered only individuals that had been followed for at least one full winter (i.e., 5 months), which included 15 caribou followed over a total of 20 winters. For individuals that were followed over multiple winters, we calculated the average value of home-range size and of the proportion of the home range made up of cutovers and road density. We thus ended up with a single estimate of each these three variables for every caribou ($n = 15$).

Quantification of Δ. We monitored 43 caribou with VHF collars (see fig. 3 of Courtois et al. 2008 for a spatial representation of their distribution over the study area), 16 of which had at least five locations per year over at least two successive years. These 16 caribou were used to test whether, following human disturbance, only individuals at or near the disturbed areas tend to move away from it. Caribou were captured between 1998 and 2005 with a net gun fired from a helicopter. Radio-collared females were located approximately every 3 weeks between November 1 and April 30 by monitoring the study area from aircraft (Navajo 350, Cessna 185, Cessna 310, or Cessna 337) equipped with two unidirectional antennas. We estimated the centroid of winter locations as in Moorcroft and Lewis (2006) for each radio-tracked caribou every year ($n = 5.0 \pm 0.4$ locations individual^{-1} year^{-1}; range: 1–16). Using the geographic information system (see "Quantification of ε"), we determined the distance between each current centroid location and the future location of the nearest cut or road that will be present the following year. We then assessed whether or not individuals that would have ended up near (<2.5 km from) a disturbed site the next year by remaining stationary (localized movements only) would have moved farther from that site, compared to individuals already located farther (≥2.5 km) from cuts or roads. This threshold provided a number of observations that was sufficient at both large and small distances to carry out statistical analysis (i.e., eight caribou with eight centroids located less than 2.5 km from cuts and roads and 14 caribou with 27 centroids located at least 2.5 km from these anthropogenic features). The comparison was performed with mixed-effects models with Gaussian distribution, with individuals being considered a random effect to account for the nonindependence of observations for caribou followed during more than one winter.

Recall that parameter Δ corresponds to the distance from the edge of the disturbance to where the boundary effect starts decaying to 0. This parameter was therefore estimated by identifying the average centroid locations of VHF-collared individuals that did not shift their activity center (i.e., centroid of their locations) when cuts or roads expanded in their direction, as indicated from the mixed-effects models.

Redistribution of Caribou Following Anthropogenic Disturbance: Model Validation

The model's prediction was tested through aerial surveys of caribou snow tracks conducted over 161,920 km^2 of boreal forest in Québec. The area is dominated by conifer forests (62%) consisting mostly of black spruce, balsam fir, and jack pine. Mean annual temperatures range between −2.5° and 0°C, and mean annual precipitation varies from 600 to 1,400 mm. The study area is subject to forest harvesting, especially south of 51.5°N (see Fortin et al. 2008 for details).

The study area was surveyed between 1999 and 2005, generally from late February to late March, by flying along transects that were evenly spaced 2.1 km apart. Each area was surveyed only once. Overall, 90% of all caribou track networks should have been detected in the study region (Courtois et al. 2003*a*). Our study thus avoids potential methodological artifacts caused by the failure to saturate the study area with collared animals. Subsequent analyses were based on these centroids of intensively used areas ($n = 401$; see Fortin et al. 2008 for an illustration of their spatial distribution). We characterized the 401 observed centroid locations, together with 4,010 locations randomly selected more than 0.5 km from the observed ones. For all locations, we determined the distance from the nearest cutblock or road and whether they occurred in a conifer forest (dominated by open or closed conifer stands with

moss), a deciduous or mixed forest, a burned area, a lake, a lichen-heath community (dominated by lichens, with 10%–40% conifers, or by shrubs and lichens), or another type (dominated by bare ground, moss and shrubs, agricultural lands, or unclassified areas). We characterized habitat covariates using the Third Québec Forest Resources Inventory (Ministère des Ressources naturelles et de la Faune du Québec) with 1–8-ha resolution. Clear-cut and road locations were overlaid on the forest map and updated every year with information provided by local forestry companies.

We evaluated edge effects by using a binomial, semiparametric generalized additive model contrasting locations with (coded as 1) and without (coded as 0) a track network. Habitat covariates (water body, lichen-heath community, conifer forest, peatland, burn, and mixed or deciduous forest) were considered independent parametric variables, whereas distance to the nearest disturbed site (clear-cut or road) was an independent nonparametric variable. This analysis was restricted to observations less than 30 km from disturbances (i.e., the ninetieth distance percentile of track networks) because most edge effects vanished farther than 10 km from the disturbance and because we encountered model convergence issues when considering the entire data set. To avoid overfitting, we modeled edge effects while considering only 5.03 df, that is, 1 for the linear term and 4.03 for the (spline) smooth term. The model did not converge when we included both clear-cut and road nonparametric variables, possibly because of the strong correlation between distance to nearest cut and distance to nearest road ($r = 0.76$; $n = 4{,}010$ random locations). We thus made models that accounted for the distance to the nearest clear-cut only, that to the nearest road only, or that to either the nearest cut or the nearest road. A similar pattern of higher probability of occurrence near disturbed sites emerged for all models (fig. B2 in app. B). We thus present only the model based on the nearest anthropogenic feature, whether cut or road.

We estimated Strauss's linear index (Strauss 1979) as (observed proportion of track network in distance bin *i*) minus (expected proportion of track networks for distance bin *i*), for all 0.5-km distance bins within the range 0–30 km (Manly et al. 2002). Expected proportions were determined on the basis of the distance distribution of random locations.

All statistical analyses were performed in SAS 9.2 (SAS Institute, Cary, NC). Data are deposited in the Dryad repository: http://dx.doi.org/10.5061/dryad.kh356.

Results

Model Parameterization

The home-range size of GPS-collared caribou averaged 958 ± 370 km^2 ($n = 15$ individuals; range: 68–5,723 km^2), as estimated from a 100% Brownian bridge kernel. The area covered by cutovers in those home ranges was 13 ± 15 km^2 ($n = 15$; range: 0–200 km^2), whereas road density averaged 0.14 ± 0.04 km km^{-2} ($n = 15$; range: 0–0.58 km km^{-2}).

The mean vector direction of GPS-collared caribou during intercamp movements was oriented away from disturbed areas for distances up to 3.7 km (fig. B1 in app. B); we thus set $\varepsilon = 3.7$ km. At greater distances, caribou tended to come back toward human disturbance, presumably because they were heading back toward their home-range center. Indeed, the median intercamp movement (i.e., 50% closer and 50% farther) of the GPS-collared individuals occurred, on average, at 4.19 ± 0.66 km ($n = 17$ caribou; median: 3.5 km; range: 1.50–10.25 km) from the nearest human-induced edge. In other words, half of the intercamp movements that ultimately define the home range (Bailey et al. 1996) occurred, on average, when caribou were located closer than 4.19 km from a cut or a road, and half occurred when individuals were located farther than that.

We found that VHF-collared caribou for which the centroid of their current locations would have been less than 2.5 km from the nearest clear-cut or road the next year if they remained stationary (i.e., with no home-range shift), moved 3.43 ± 0.92 km (mean ± SE) away from that site ($t = 3.74$, $P = .007$, $n = 8$ caribou, 8 centroids), which resulted in their new centroids being 4.25 ± 1.09 km from any human disturbances. In contrast, individuals already located farther from those sites did not move systematically with regard to the disturbance ($t = -0.30$, $P = .77$, $n = 14$ caribou, 27 centroids). The centroids of these 14 caribou occurred at 7.43 ± 1.22 km, and we thus set $\Delta = 7.4$ km (see app. A).

Model Prediction

With these parameter estimates, the model predicts that the highest density of caribou should occur 3.7 km from roads or clear-cuts (fig. 1). This peak is caused by a shift in home range location by some individuals in response to the disturbance, reinforced by a general propensity for moving away from the disturbance while remaining within the home range.

Redistribution of Caribou Following Anthropogenic Disturbance: Model Validation

As the advection-diffusion model predicts, the distribution of track networks recorded over 161,920 km^2 was heavily skewed toward human-disturbed sites (skewness = 1.14, which exceeded 0 skewness; $P < .001$, $n = 401$; fig. 2*A*), with the distribution tail reaching 48.1 km. After con-

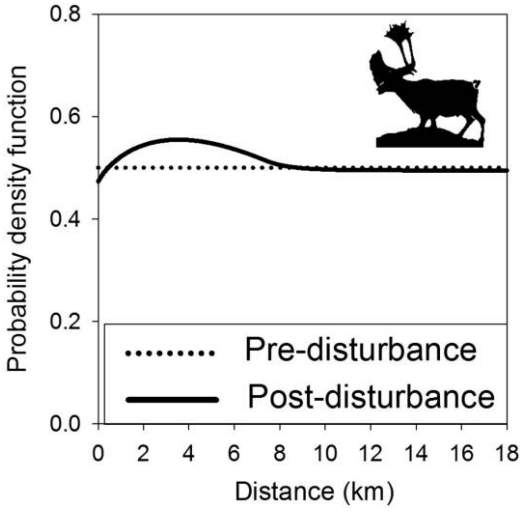

Figure 1: Expected redistribution of woodland caribou following anthropogenic disturbance, as predicted from an advection-diffusion movement model. The simulations are based on $\rho_0 = 4$, $b = 0.183$, $\varepsilon = 3.7$, $\Delta = 7.4$, which were estimated from radio-collared caribou followed in the boreal forest of the Côte-Nord region of Québec, Canada. The edge of the nearest anthropogenic feature occurs at 0 km.

trolling for other habitat features (table 1), we observed that the relative probability of observing a track network was lowest directly at anthropogenic disturbance boundaries and increased toward a maximum at 4.45 km before decreasing in an oscillatory manner to an intermediate probability level (fig. 2*B*). This empirical peak thus closely matches the quantitative prediction (i.e., 3.7 km) of our model parameterized from a completely independent data set.

Discussion

We developed a mechanistic model of edge effects that uses basic behavioral mechanisms to predict that the redistribution of animals negatively affected by human disturbance can result in their abundance being highest in the vicinity of disturbed areas. This prediction rests on three key behaviors: (1) animals located in or near a disturbed site move away—but at a limited distance—from the site once it is disturbed, (2) animals already established farther away do not relocate their home range, and (3) animals remain away because of distance-dependent directional biases and home-range behavior. These responses are commonly reported for a broad range of animal species: reaction to habitat boundary (e.g., Desrochers and Fortin 2000; Schultz and Crone 2001; Morales 2002; Moorcroft and Lewis 2006; Moorcroft et al. 2006), limited dispersal distances (reviewed in Sutherland et al. 2000), and movement biases with respect to anthropogenic features (e.g., Dyer et al. 2002; Fortin et al. 2005; Rand et al. 2006; Van Houtan et al. 2007). The redistribution in response to human-induced edges reported here should therefore be representative of a broad range of vagile species. In this study, we provide empirical evidence that all three behaviors reflect the response of forest-dwelling caribou to human disturbance. First, caribou located less than 2.5 km from a clear-cut or a road moved away once the site was disturbed. They reestablished their activity centers 4.25 km from the nearest cut or road. Second, animals already located at least 2.5 km away did not shift their home-range location with respect to the disturbed sites. The absence of response to the local increase in conspecific density could be explained by the abundance of food resources. Indeed, forest-dwelling caribou generally occur at a density approximately one-third to one-fourth (Courtois et al. 2007, 2008; Courbin et al. 2009) that required to experience food limitation (Courtois et al. 2007). Third, when caribou were established away from cuts and roads, they remained at a distance by adjusting their movements with respect to the disturbed areas.

Based on these behavioral mechanisms, the advection-diffusion movement model predicted a nonmonotonic functional form of edge effects, with a maximum density of caribou occurring at 3.7 km from roads or clear-cuts, that is, where the propensity for moving away from the disturbance is counterbalanced by that for staying within the home range. In fact, the steady state probability distribution peaks at ε, which is an equilibrium distance in the vector field $\mathbf{V}_\varepsilon(\mathbf{x})$. This situation will occur whenever $\varepsilon < \Delta$. The peak should persist as long as the marginal fitness gains of site fidelity remain higher than the marginal fitness costs of crowding. In forest ecosystems, however, the peak should eventually disappear in cutovers as harvested stands return to their prelogging conditions. Reaching these conditions should take many years because caribou still respond negatively to cutovers after 50–70 years (Hins et al. 2009). When $\varepsilon \geq \Delta$, the individual's motion is away from the boundary until the edge effect dissipates, and the model would not show a peak at steady state. The peak will simply be a transient property of movement decisions.

The predicted nonmonotonic response of animals to human-induced edges was consistent with field observations of caribou distribution over 161,920 km^2. Moreover, the area of highest activity predicted near cuts or roads by our PDE model matched rather closely the observed maximum probability of caribou occurrence, which occurred at 4.5 km (availability: 0–85 km) away from these anthropogenic features. This peak was also consistent with the peak in caribou abundance 4–10 km away from surface developments on the rugged terrain (though not on flat

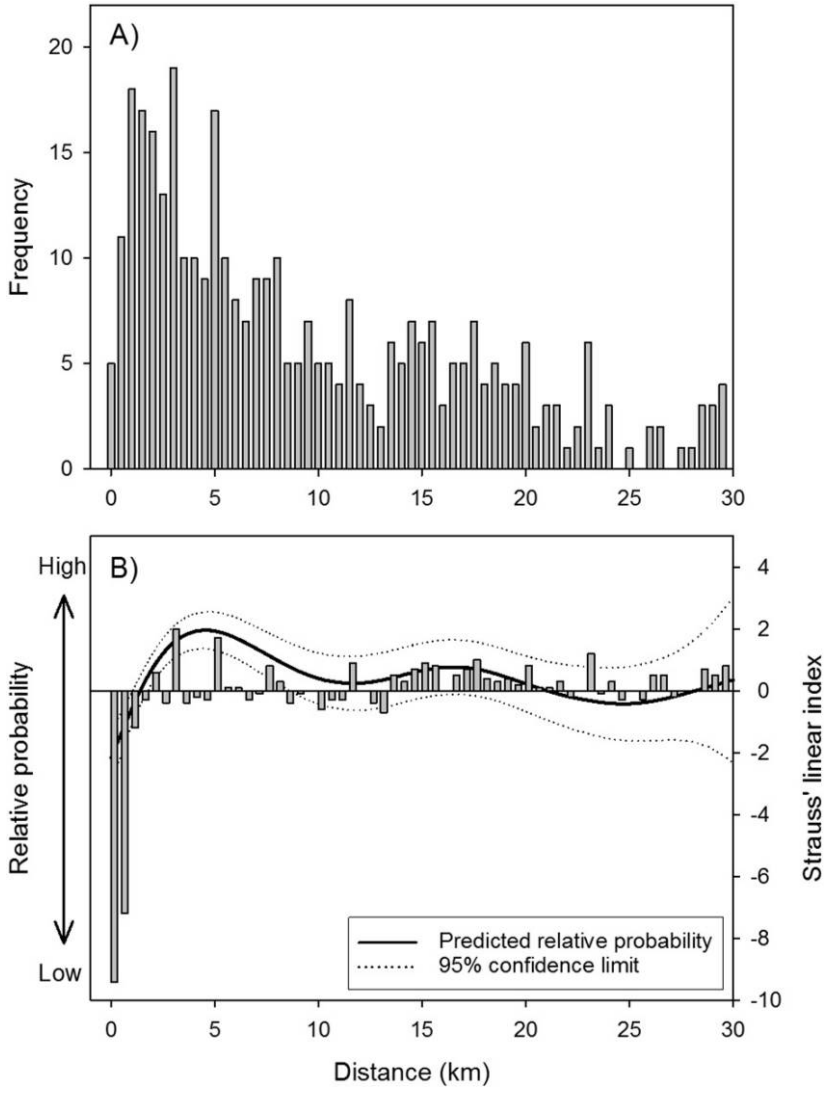

Figure 2: *A*, Frequency distribution of distance from nearest clear-cut or road within the 0–30-km range (maximum distance of observed tracks, 48 km) for track networks of woodland caribou observed over 161,920 km^2 of boreal forest in Québec, Canada. *B*, Relative probability of occurrence of caribou track networks in winter as a function of the distance from the nearest anthropogenic disturbance, overlaid with Strauss's linear index estimated for 0.5-km distance classes. A negative bar implies that the proportion of observed tracks was less than random expectation.

terrain) of Alaska reported by Nellemann and Cameron (1996). Other studies have reported that caribou abundance increases with distance from human disturbances (Nellemann et al. 2001, 2003; Johnson et al. 2005). These studies, however, did not evaluate the possibility of a decrease more than 10 km from disturbed sites (Nellemann et al. 2001, 2003) or discarded this pattern if observed (Johnson et al. 2005). In fact, most investigations occur over a spatial domain that is too restricted to fully appreciate the extent of edge effects (Ewers and Didham 2008).

The nonmonotonic response to edges reported here is not expected from classical edge-effect theory, and it can imply fundamental differences in ecological patterns and processes, such as in the spatial organization of biodiversity and the spatial structure of trophic interactions. For example, local maxima in prey density could increase local predation risk because predators can then focus their hunt in those areas. Indeed, predators are commonly drawn to areas where their prey aggregate (Mao et al. 2005; McPhee et al. 2012). Moreover, the preferences of generalist predators is a function of the relative abundance of multiple

Table 1: Semiparametric generalized additive model of habitat selection by woodland caribou in winter

	β	SE	t	P	df	Sum of squares	χ^2
Covariate:							
Water body	1.128	.250	4.51	<.0001			
Lichen-heath community	1.035	.272	3.81	.0001			
Conifer forest	.644	.223	2.89	.004			
Peatland	.503	.294	1.71	.09			
Burn	−1.218	.618	−1.97	.05			
Mixed forest	−3.741	3.390	−1.10	.27			
Road	−3.323	3.007	−1.08	.28			
Linear (D)	.046	.007	6.28	<.0001			
Analysis of deviance:							
Spline (D) source				<.0001	4.03	49.57	49.60

Note: The model is based on a comparison between the characteristics of centroids of track networks located from aerial surveys conducted between 1999 and 2005 over a 161,920-km^2 section of the boreal forest, Québec, Canada. The analysis of deviance indicates the relevance of considering nonlinear effects of distance from the nearest anthropogenic disturbance (D, in km) on the relative probability of occurrence of track networks. Selection coefficients (β) are presented with standard errors (SE) and associated P values. The habitat selection model presented here was a strong improvement over the null model, which consisted of the intercept only (log-likelihood ratio test: $\chi^2 = 191$, df = 12.03, $P < .0001$). "Clear-cut" was the reference category.

prey species (e.g., Murdoch 1969; Steenhof and Kochert 1988; Siddon and Witman 2004; Garrott et al. 2007). Species-specific responses of prey to habitat edges (Sauvajot et al. 1998; Frair et al. 2005; Johnson et al. 2005; Ngoprasert et al. 2007; Jiang et al. 2008) can lead to spatial variation in the encounter rates of predators with certain prey species, which may result in predators targeting different prey in different parts of the landscape. Such prey-switching behavior is recognized as a critical process driving the dynamics of predator-prey systems (van Baalen et al. 2001; Kimbrell and Holt 2005). The spatial structure in predator-prey interactions appears more likely to emerge when edge effects induce nonmonotonic prey distributions than when local prey concentrations are not expected, as with the current edge-effect paradigm.

In an increasingly fragmented world (Watts et al. 2007), understanding human-induced edge effects is becoming urgent. The response to edges shapes a wide range of processes, such as herbivory, predation, and parasitism rates, with direct implications for biological control and conservation biology (Ewers and Didham 2006; Wimp et al. 2011). Evaluation of edge effects should consider nonmonotonic responses because they can entail profound differences in food-web dynamics and ecosystem functioning relative to expectations from classical theories. In the case of forest-dwelling caribou, aggregation near a disturbance provides predators with an area on which to focus their hunt, which is not expected from the classical view. Our advection-diffusion model offers a mechanistic explanation for this pattern, thereby providing a new look at edge effects in human-altered landscapes.

Acknowledgments

This work was supported by Natural Sciences and Engineering Research Council (NSERC)–Université Laval industrial research chairs (D.F., A.F.), an NSERC discovery grant (P.L.B., A.F., D.F.), Fonds de recherche du Québec–nature et technologies (D.F.), an NSERC Undergraduate Student Research Award (C.T.G.), and the University of Ontario Institute of Technology (P.L.B.), as well as the Ministère des Ressources naturelles du Québec. We are grateful to J. Morales, W. Parsons, and A. Vanak for providing comments on this article and to J. Deteix and C. Tibirna for help with the numerical simulations.

Literature Cited

Bailey, D. W., J. E. Gross, E. A. Laca, L. R. Rittenhouse, M. B. Coughenour, D. M. Swift, and P. L. Sims. 1996. Mechanisms that result in large herbivore grazing distribution patterns. Journal of Range Management 49:386–400.

Baker, J., K. French, and R. J. Whelan. 2002. The edge effect and ecotonal species: bird communities across a natural edge in southern Australia. Ecology 83:3048–3059.

Barraquand, F., and S. Benhamou. 2008. Animal movements in heterogeneous landscapes: identifying profitable places and homogeneous movement bouts. Ecology 89:3336–3348.

Bastille-Rousseau, G., D. Fortin, C. Dussault, R. Courtois, and J.-P. Ouellet. 2011. Foraging strategies by omnivores: are black bears actively searching for ungulate neonates or are they simply opportunistic predators? Ecography 34:588–596.

Boyce, M. S. 2006. Scale for resource selection functions. Diversity and Distributions 12:269–276.

Boyce, M. S., and L. L. McDonald. 1999. Relating populations to

habitats using resource selection functions. Trends in Ecology and Evolution 14:268–272.

Boyce, M. S., and J. S. Waller. 2003. Grizzly bears for the Bitterroot predicting potential abundance and distribution. Wildlife Society Bulletin 31:670–683.

Brodeur, V., J.-P. Ouellet, R. Courtois, and D. Fortin. 2008. Habitat selection by black bears in an intensively logged boreal forest Canadian Journal of Zoology 86:1307–1316.

Ciucci, P., M. Masi, and L. Boitani. 2003. Winter habitat and travel route selection by wolves in the northern Apennines, Italy. Ecography 26:223–235.

Courbin, N., D. Fortin, C. Dussault, and R. Courtois. 2009. Landscape management for woodland caribou: the protection of forest blocks influences wolf-caribou co-occurrence. Landscape Ecology 24:1375–1388.

Courtois, R., A. Gingras, C. Dussault, L. Breton, and J. P. Ouellet 2003*a*. An aerial survey technique for the forest-dwelling ecotype of woodland caribou, *Rangifer tarandus caribou*. Canadian Field-Naturalist 117:546–554.

Courtois, R., A. Gingras, D. Fortin, A. Sebbane, B. Rochette, and L. Breton. 2008. Demographic and behavioural response of woodland caribou to forest harvesting. Canadian Journal of Forest Researcl 38:2837–2849.

Courtois, R., J. P. Ouellet, L. Breton, A. Gingras, and C. Dussault. 2007. Effects of forest disturbance on density, space use, and mortality of woodland caribou. Écoscience 14:491–498.

Courtois, R., J. P. Ouellet, A. Gingras, C. Dussault, L. Breton, and J. Maltais. 2003*b*. Historical changes and current distribution of caribou, *Rangifer tarandus*, in Quebec. Canadian Field-Naturalist 117: 399–414.

Crête, M., and R. Courtois. 1997. Limiting factors might obscure population regulation of moose (Cervidae: *Alces alces*) in unproductive boreal forests. Journal of Zoology 242:765–781.

Desrochers, A., and M. J. Fortin. 2000. Understanding avian responses to forest boundaries: a case study with chickadee winter flocks. Oikos 91:376–384.

Dyer, S. J., J. P. O'Neill, S. M. Wasel, and S. Boutin. 2002. Quantifying barrier effects of roads and seismic lines on movements of female woodland caribou in northeastern Alberta. Canadian Journal of Zoology 80:839–845.

Eigenbrod, F., S. J. Hecnar, and L. Fahrig. 2009. Quantifying the road-effect zone: threshold effects of a motorway on anuran populations in Ontario, Canada. Ecology and Society 14:24.

Ewers, R. M., and R. K. Didham. 2006. Confounding factors in the detection of species responses to habitat fragmentation. Biological Reviews 81:117–142.

———. 2007. The effect of fragment shape and species' sensitivity to habitat edges on animal population size. Conservation Biology 21:926–936.

———. 2008. Pervasive impact of large-scale edge effects on a beetle community. Proceedings of the National Academy of Sciences of the USA 105:5426–5429.

Ewers, R. M., S. Thorpe, and R. K. Didham. 2007. Synergistic interactions between edge and area effects in a heavily fragmented landscape. Ecology 88:96–106.

Forman, R. T. T., and L. E. Alexander. 1998. Roads and their major ecological effects. Annual Review of Ecology and Systematics 29: 207–231.

Fortin, D., H. L. Beyer, M. S. Boyce, D. W. Smith, T. Duchesne, and J. S. Mao. 2005. Wolves influence elk movements: behavior shapes a trophic cascade in Yellowstone National Park. Ecology 86:1320–1330.

Fortin, D., R. Courtois, P. Etcheverry, C. Dussault, and A. Gingras. 2008. Winter selection of landscapes by woodland caribou: behavioural response to geographical gradients in habitat attributes. Journal of Applied Ecology 45:1392–1400.

Frair, J. L., E. H. Merrill, D. R. Visscher, D. Fortin, H. L. Beyer, and J. M. Morales. 2005. Scales of movement by elk (*Cervus elaphus*) in response to heterogeneity in forage resources and predation risk. Landscape Ecology 20:273–287.

Fryxell, J. M., M. Hazell, L. Börger, B. D. Dalziel, D. T. Haydon, J. M. Morales, T. McIntosh, and R. C. Rosatte. 2008. Multiple movement modes by large herbivores at multiple spatiotemporal scales. Proceedings of the National Academy of Sciences of the USA 105: 19114–19119.

Garrott, R. A., J. E. Bruggeman, M. S. Becker, S. T. Kalinowski, and P. J. White. 2007. Evaluating prey switching in wolf-ungulate systems. Ecological Applications 17:1588–1597.

Girvetz, E. H., J. A. G. Jaeger, and J. H. Thorne. 2007. Comment on "Roadless Space of the Conterminous United States". Science 318: 1240b.

Hins, C., J. P. Ouellet, C. Dussault, and M.-H. St-Laurent. 2009. Habitat selection by forest-dwelling caribou in managed boreal forest of eastern Canada: evidence of a landscape configuration effect. Forest Ecology and Management 257:636–643.

Horne, J. S., E. O. Garton, S. M. Krone, and J. S. Lewis. 2007. Analyzing animal movements using Brownian bridges. Ecology 88: 2354–2363.

Houle, M., D. Fortin, C. Dussault, R. Courtois, and J.-P. Ouellet. 2010. Cumulative effects of forestry on habitat use by gray wolf (*Canis lupus*) in the boreal forest. Landscape Ecology 25:419–433.

Jiang, G. S., M. H. Zhang, and J. Z. Ma. 2008. Habitat use and separation between red deer *Cervus elaphus xanthopygus* and roe deer *Capreolus pygargus bedfordi* in relation to human disturbance in the Wandashan Mountains, northeastern China. Wildlife Biology 14:92–100.

Johnson, C. J., M. S. Boyce, R. L. Case, H. D. Cluff, R. J. Gau, A. Gunn, and R. Mulders. 2005. Cumulative effects of human developments on arctic wildlife. Wildlife Monographs 160:1–36.

Johnson, D. H. 1980. The comparison of usage and availability measurements for evaluating resource preference. Ecology 61:65–71.

Kimbrell, T., and R. D. Holt. 2005. Individual behaviour, space and predator evolution promote persistence in a two-patch system with predator switching. Evolutionary Ecology Research 7:53–71.

Manly, B. F. J., L. L. McDonald, D. L. Thomas, T. L. McDonald, and W. P. Erickson. 2002. Resource selection by animals: statistical design and analysis for field studies. Kluwer Academic, Dordrecht.

Mao, J. S., M. S. Boyce, D. W. Smith, F. J. Singer, D. J. Vales, J. M. Vore, and E. H. Merrill. 2005. Habitat selection by elk before and after wolf reintroduction in Yellowstone National Park. Journal of Wildlife Management 69:1691–1707.

McPhee, H. M., N. F. Webb, and E. H. Merrill. 2012. Hierarchical predation: wolf (*Canis lupus*) selection along hunt paths and at kill sites. Canadian Journal of Zoology 90:555–563.

Moorcroft, P. R., and M. A. Lewis. 2006. Mechanistic home range analysis. Monographs in Population Biology 43. Princeton University Press, Princeton, NJ.

Moorcroft, P. R., M. A. Lewis, and R. L. Crabtree. 2006. Mechanistic home range models capture spatial patterns and dynamics of coy-

ote territories in Yellowstone. Proceedings of the Royal Society B Biological Sciences 273:1651–1659.

Morales, J. M. 2002. Behavior at habitat boundaries can produc leptokurtic movement distributions. American Naturalist 160:531–538.

Moreau, G., D. Fortin, S. Couturier, and T. Duchesne. 2012. Multi-level functional responses for wildlife conservation: the case of threatened caribou in managed boreal forests. Journal of Applie Ecology 49:611–620.

Murdoch, W. W. 1969. Switching in general predators: experiments on predator specificity and stability of prey populations. Ecologica Monographs 39:335–354.

Nellemann, C., and R. D. Cameron. 1996. Effects of petroleum development on terrain preferences of calving caribou. Arctic 49:23–28.

Nellemann, C., I. Vistnes, P. Jordhoy, and O. Strand. 2001. Winter distribution of wild reindeer in relation to power lines, roads and resorts. Biological Conservation 101:351–360.

Nellemann, C., I. Vistnes, P. Jordhoy, O. Strand, and A. Newton. 2003. Progressive impact of piecemeal infrastructure development on wild reindeer. Biological Conservation 113:307–317.

Ngoprasert, D., A. J. Lynam, and G. A. Gale. 2007. Human distur bance affects habitat use and behaviour of Asiatic leopard *Panthera pardus* in Kaeng Krachan National Park, Thailand. Oryx 41:343–351.

Pinard, V., C. Dussault, J.-P. Ouellet, D. Fortin, and R. Courtois. 2012. Calving rate, calf survival rate and habitat selection of forest-dwelling caribou in a highly managed landscape. Journal of Wild life Management 76:189–199.

Rand, T. A., J. M. Tylianakis, and T. Tscharntke. 2006. Spillover edge effects: the dispersal of agriculturally subsidized insect natural en emies into adjacent natural habitats. Ecology Letters 9:603–614.

Reeve, J. D., and J. T. Cronin. 2010. Edge behaviour in a minute parasitic wasp. Journal of Animal Ecology 79:483–490.

Ries, L., R. J. Fletcher, J. Battin, and T. D. Sisk. 2004. Ecologica responses to habitat edges: mechanisms, models, and variability explained. Annual Review of Ecology Evolution and Systematics 35:491–522.

Ries, L., and T. D. Sisk. 2004. A predictive model of edge effects. Ecology 85:2917–2926.

Sauvajot, R. M., M. Buechner, D. A. Kamradt, and C. M. Schonewald. 1998. Patterns of human disturbance and response by small mammals and birds in chaparral near urban development. Urban Ecosystems 2:279–297.

Schaefer, J. A. 2003. Long-term range recession and the persistence of caribou in the taiga. Conservation Biology 17:1435–1439.

Schultz, C. B., and E. E. Crone. 2001. Edge-mediated dispersal behavior in a prairie butterfly. Ecology 82:1879–1892.

Siddon, C. E., and J. D. Witman. 2004. Behavioral indirect interactions: multiple predator effects and prey switching in the rocky subtidal. Ecology 85:2938–2945.

Steenhof, K., and M. N. Kochert. 1988. Dietary responses of three raptor species to changing prey densities in a natural environment. Journal of Animal Ecology 57:37–48.

Strauss, R. E. 1979. Reliability estimates for Ivlev's electivity index, the forage ratio, and a proposed linear index of food selection. Transactions of the American Fisheries Society 108:344–352.

Sutherland, G. D., A. S. Harestad, K. Price, and K. P. Lertzman. 2000. Scaling of natal dispersal distances in terrestrial birds and mammals. Conservation Ecology 4:16.

Thomas, D. C., and D. R. Gray. 2002. Update COSEWIC status report on the woodland caribou *Rangifer tarandus caribou* in Canada, *in* COSEWIC assessment and update status report on the woodland caribou *Rangifer tarandus caribou* in Canada. Committee on the Status of Endangered Wildlife in Canada, Ottawa.

van Baalen, M., V. Křivan, P. C. J. van Rijn, and M. W. Sabelis. 2001. Alternative food, switching predators, and the persistence of predator-prey systems. American Naturalist 157:512–524.

Van Houtan, K. S., S. L. Pimm, J. M. Halley, R. O. Bierregaard Jr., and T. E. Lovejoy. 2007. Dispersal of Amazonian birds in continuous and fragmented forest. Ecology Letters 10:219–229.

Watts, R. D., R. W. Compton, J. H. McCammon, C. L. Rich, S. M. Wright, T. Owens, and D. S. Ouren. 2007. Roadless space of the conterminous United States. Science 316:736–738.

Whittington, J., M. Hebblewhite, N. J. DeCesare, L. Neufeld, M. Bradley, J. Wilmshurst, and M. Musiani. 2011. Caribou encounters with wolves increase near roads and trails: a time-to-event approach. Journal of Applied Ecology 48:1535–1542.

Wimp, G. M., S. M. Murphy, D. Lewis, and L. Ries. 2011. Do edge responses cascade up or down a multi-trophic food web? Ecology Letters 14:863–870.

Wittmer, H. U., B. N. McLellan, R. Serrouya, and C. D. Apps. 2007. Changes in landscape composition influence the decline of a threatened woodland caribou population. Journal of Animal Ecology 76:568–579.

Associate Editor: Wolf M. Mooij
Editor: Judith L. Bronstein

 DOI: 10.1086/670243

Appendix A from D. Fortin et al., "Movement Responses of Caribou to Human-Induced Habitat Edges Lead to Their Aggregation near Anthropogenic Features"

(Am. Nat., vol. 181, no. 6, p. 827)

Detailed Description of the Advection-Diffusion Movement Model

The partial differential $\partial v(\mathbf{x}, \mathbf{t})/\partial t = \nabla \cdot [(\rho_0^2/2)\nabla v] - \nabla \cdot [(\rho_0^2/2)b\mathbf{V}_\varepsilon(\mathbf{x})v]$ is a Fokker-Planck equation, an advection-diffusion model describing the time evolution of the location of caribou in a given domain, expressed as a probability density function. The magnitude and direction of the advection term reflect preferential movement by individuals, as given by the vector field $\mathbf{V}_\varepsilon(\mathbf{x})$, which depends on the location of the nearest boundary between forested and deforested regions and the size of the caribou's home range. The parameter ε is the distance at which the repulsive effect of the edge of the disturbance vanishes.

Vector Field $\mathbf{V}_\varepsilon(\mathbf{x})$

Let $\mathbf{x}_b = (x_b, y_b)$ be the point at the edge of the deforested region closest to $\mathbf{x}$. We define the following vectors based at $\mathbf{x}$. Let $\delta(\mathbf{x}) = \|\mathbf{x}_b - \mathbf{x}\|$; then,

$$\mathbf{v}_b = \frac{\mathbf{x}_b - \mathbf{x}}{\delta(\mathbf{x})} = \frac{(x_b - x, y_b - y)}{\delta(\mathbf{x})} = (\cos\phi_b, \sin\phi_b),$$

where $\phi_b = \arctan((y_b - y)/(x_b - x))$.

We use the logarithmic fit of the average direction taken by caribou as a function of the distance shown in figure B1 to characterize the movement model. Let $\varepsilon = 3.7$, and we set $\Delta = 7.4$ as a threshold value:

$$\mu_\varepsilon(\delta(\mathbf{x})) = \begin{cases} -\alpha \ln(\delta(\mathbf{x})) + \beta) + \gamma & \delta(\mathbf{x}) < \Delta, \\ y^* \exp(-10(\delta(\mathbf{x}) - \Delta)) & \delta(\mathbf{x}) \geq \Delta, \end{cases} \tag{A1}$$

where $\alpha = 0.17$, $\beta = \exp((\gamma - 1)/\alpha)$, $\gamma = \alpha \ln(\varepsilon/(1 - \exp(-1/\alpha)))$, and $y^* = -\alpha \ln(\Delta + \beta) + \gamma$.

Consider now the angle $\phi_+^\varepsilon := \phi_b + \pi/2 + \mu_\varepsilon(\delta(\mathbf{x}))(\pi/2)$. We define the vectors

$$\mathbf{v}_{\varphi+}^\varepsilon := (\cos\varphi_+^\varepsilon, \sin\varphi_+^\varepsilon)$$

and

$$(\mathbf{v}_{\varphi+}^\varepsilon)^\perp = (\cos(\varphi_+^\varepsilon + \pi/2), \sin(\varphi_+^\varepsilon + \pi/2)) = (-\sin\varphi_+^\varepsilon, \cos\varphi_+^\varepsilon).$$

Let

$$V_{\phi+} = \frac{1}{2}(1 + \operatorname{sgn}\delta(\mathbf{x}))v_{\phi+}^\varepsilon,$$

$$V_{\phi+}^\perp = \frac{1}{2}(1 + \operatorname{sgn}\delta(\mathbf{x}))(v_{\phi+}^\varepsilon)^\perp,$$

$$V_b = \frac{1}{2}(1 - \operatorname{sgn}\delta(\mathbf{x}))v_b.$$

Define

$$\mathbf{V}_\varepsilon(\mathbf{x}) = (\psi - (1 - \psi)\cos(\mu_\varepsilon(\delta(\mathbf{x})\pi))V_{\phi+}) + (1 - \psi)\sin(\mu_\varepsilon(\delta(\mathbf{x}))\pi)V_{\phi+}^\perp - V_b,$$

where $\psi \in [0,1]$ is a parameter giving the direction bias. In all the numerical simulations, we set $\psi = 0.5$ (this choice of value is justified in "Derivation of the Equation"). Thus, we have

$$\mathbf{V}_\varepsilon(\mathbf{x}) = 0.5(1 - \cos(\mu_\varepsilon(\delta(\mathbf{x})\pi))V_{\phi+}) + 0.5\sin(\mu_\varepsilon(\delta(\mathbf{x})\pi))V_{\phi+}^\perp - V_b.$$

It is convenient, particularly for computer implementation, to write $\mathbf{v}^{\varepsilon}_{\phi+}$ and $(\mathbf{v}^{\varepsilon}_{\phi+})^{\perp}$ in terms of $\mathbf{v}_b$ as follows:

$$\mathbf{v}^{\varepsilon}_{\phi+} = (\mathbf{v}_b \cdot (-\sin(\mu_\varepsilon(\delta(\mathbf{x}))\pi/2)),\ -\cos(\mu_\varepsilon(\delta(\mathbf{x}))\pi/2), \mathbf{v}_b \cdot (\cos(\mu_\varepsilon(\delta(\mathbf{x}))\pi/2),\ -\sin(\mu_\varepsilon(\delta(\mathbf{x}))\pi/2))),$$

$$(\mathbf{v}^{\varepsilon}_{\phi+})^{\perp} = (\mathbf{v}_b \cdot (-\cos(\mu_\varepsilon(\delta(\mathbf{x}))\pi/2)),\ \sin(\mu_\varepsilon(\delta(\mathbf{x}))\pi/2), \mathbf{v}_b \cdot (-\sin(\mu_\varepsilon(\delta(\mathbf{x}))\pi/2),\ -\cos(\mu_\varepsilon(\delta(\mathbf{x}))\pi/2))).$$

A calculation shows that

$$\mathbf{V}_\varepsilon(\mathbf{x}) = a_\varepsilon(\delta(\mathbf{x}))\mathbf{v}_b.$$

where $a_\varepsilon(\delta(\mathbf{x})) := -\sin(\mu_\varepsilon(\delta(\mathbf{x}))\pi/2)$. Because advection is in the $\mathbf{v}_b$ direction, without loss of generality, we can project onto the vector $\mathbf{v}_b$ numerical solutions computed on a two-dimensional domain.

Boundary Conditions

The advection-diffusion equation (1) is defined in a two-dimensional region Ω and has the form

$$\frac{\partial u(\mathbf{x}, t)}{\partial t} = \nabla \cdot (d(\mathbf{x})\nabla u) + \nabla \cdot (c(\mathbf{x})u) := \nabla \cdot H(\mathbf{x}, t). \tag{A2}$$

Where $u(\mathbf{x}, t)$ is a probability density function in the domain Ω, we thus need $\int_\Omega u(\mathbf{x}, t)dx = 1$ for all $t \geq 0$. In particular, a straightforward application of Green's theorem shows that $\int_\Omega u(\mathbf{x}, t)dx$ is constant for all $t \geq 0$ if the boundary condition

$$H(\mathbf{x}, t) \cdot \mathbf{N} = 0 \tag{A3}$$

is satisfied, where $\mathbf{N}$ is the unit normal vector to the boundary of Ω. Thus, for equation (1), we have

$$\nabla u - b\mathbf{V}_\varepsilon(\mathbf{x})u = 0$$

for $\mathbf{x} \in \partial\Omega$.

Estimation of Parameters Using Field Data

Estimation of the parameters of the probability density functions used the data collected on caribou with GPS collars in the Côte-Nord region of Québec, Canada. Step-length values are split into 20 bins from 0–1 km up to 19–20 km. Bins and frequency values were entered in MATLAB's "dfittool" package, and an exponential probability density was fitted to the data that were obtained, with a mean at 3.96 km; thus, we fix $\rho_0 = 4$.

The estimation of b was done as in Moorcroft and Lewis (2006). Because we assumed that the concentration parameter $\kappa = b\rho_0$ is independent of distance, it could be estimated by choosing an arbitrary distance. We chose the interval 5–6 km to compute the mean vector (r) of turning angles: $r \approx 0.344$. The concentration $\hat{\kappa}$ was estimated using the approximation $\hat{\kappa} \approx 2r + r^3 + 5r^5/6$, and we obtained $\hat{\kappa} \approx 0.733$. Thus, we set $b = 0.183$.

Derivation of the Equation

We built a random model for the movement of a caribou from location $\mathbf{x}'$ to location $\mathbf{x}$. Let f_τ be an exponential distribution with parameter λ,

$$f_\tau(\rho) = \lambda e^{-\lambda\rho},$$

where $\rho = \|\mathbf{x}' - \mathbf{x}\|$ and K_τ is a von Mises probability density,

$$K_\tau(\phi, \hat{\phi}) = \frac{1}{2\pi I_0(\kappa_\tau)} \exp(\kappa_\tau \cos(\phi - \hat{\phi})),$$

where I_0 is a modified Bessel function and κ_τ is the concentration coefficient.

The modeling assumption on mean angles is guided by the analysis of the data described in figure B1. We suppose that at a distance $\delta(\mathbf{x})$ from the edge of the disturbance, the mean angle taken by a caribou is perpendicular to the disturbance. This is described by the angles $\phi^{\varepsilon}_{\pm}(\mathbf{x})$, where

$$\hat{\phi}^{\varepsilon}_{\pm}(\mathbf{x}) = \begin{cases} \phi_b \pm \dfrac{\pi}{2} \pm \mu_\varepsilon(\delta(\mathbf{x}))\dfrac{\pi}{2} & \delta(\mathbf{x}) \geq 0, \\ \phi_b & \delta(\mathbf{x}) < 0. \end{cases}$$

We chose to model the movement behavior using a weighted sum of von Mises densities. We set the probability density function modeling the movement of caribou from $\mathbf{x}'$ to $\mathbf{x}$ with step duration τ at time t to be

$$k(\mathbf{x}', \mathbf{x} - \mathbf{x}', \tau, t) = \frac{1}{\rho} f_\tau(\rho)[\psi K_\tau(\phi, \hat{\phi}^\varepsilon_+(\mathbf{x})) + (1 - \psi) K_\tau(\phi, \hat{\phi}^\varepsilon_-(\mathbf{x}))], \tag{A4}$$

where $\psi \in [0, 1]$. Note that $\rho^{-1}(\mathbf{x}' - \mathbf{x}) = (\cos\phi, \sin\phi)$. The choice of $\psi = 0.5$ implies bilateral symmetry in the mean orientation with respect to vector $\mathbf{v}_b$. This assumption is justified because the mean bearing direction of radio-collared caribou was nearly as often biased toward the left side as toward the right side of $\mathbf{v}_b$ (i.e., 7 for ϕ_- and 5 for ϕ_+) among the categories of distance from disturbance. In other words, caribou did not display preferences for left or right turns.

Let $\bar{\rho}_\tau$ be the first moment of f_τ: we model the first moment by $\bar{\rho}_\tau = \tau^{1/2}\rho_0$, where $\rho_0 > 0$ is a parameter. Since f_τ is an exponential density, then the second moment $\overline{\rho_\tau^2}$ satisfies the first equality:

$$\overline{\rho_\tau^2} = 2\bar{\rho}_\tau^2 = 2\tau\rho_0^2.$$

Given the modeling assumptions made above, we set the concentration factor for K_τ as $\kappa_\tau = b\bar{\rho}_\tau$. The coefficient b is the directional bias per unit distance moved.

Computation of the Coefficients

Let $u(\mathbf{x}, t)$ be the probability density function of finding a caribou at location $\mathbf{x}$ and time t. The derivation of the Fokker-Planck equation describing the time evolution of $u(\mathbf{x}, t)$ is well known, and details can be found in Moorcroft and Lewis (2006). One obtains

$$\frac{\partial u}{\partial t} + \nabla \cdot (c^\varepsilon(\mathbf{x}, t)u) = \frac{\partial^2 d_{xx}(\mathbf{x}, t)u}{\partial x^2} + \frac{\partial^2 d_{xy}(\mathbf{x}, t)u}{\partial x \partial y} + \frac{\partial^2 d_{yx}(\mathbf{x}, t)u}{\partial y \partial x} + \frac{\partial^2 d_{yy}(\mathbf{x}, t)u}{\partial y^2},$$

where the advection term $c^\varepsilon(\mathbf{x}, t)$ and the diffusion coefficients d are expressed in terms of an integral (Moorcroft and Lewis 2006). The coefficient $c^\varepsilon(\mathbf{x}, t)$ depends on the location $\mathbf{x}$ with respect to the nearest boundary between forested and deforested regions: (1) if $\delta(\mathbf{x}) < 0$, then $c^\varepsilon = |c^\varepsilon|\mathbf{v}_b$, and (2) if $0 \le \delta(\mathbf{x})$, then we have

$$c^\varepsilon(\mathbf{x}, t) = \lfloor c^\varepsilon(\mathbf{x}, t) \cdot \mathbf{v}^\varepsilon_{\phi+} \rfloor \mathbf{v}^\varepsilon_{\phi+} + \lfloor c^\varepsilon(\mathbf{x}, t) \cdot (\mathbf{v}^\varepsilon_{\phi+})^\perp \rfloor (\mathbf{v}^\varepsilon_{\phi+})^\perp.$$

Thus, we need only to compute explicitly $c(\mathbf{x}, t) \cdot \mathbf{v}_b$, $c(\mathbf{x}, t) \cdot \mathbf{v}^\varepsilon_{\phi+}$, and $c(\mathbf{x}, t) \cdot (\mathbf{v}^\varepsilon_{\phi+})^\perp$. The following identities are useful in the computations below. In cases 1 and 2, we need

$$\mathbf{v}_b \cdot \frac{\mathbf{x}' - \mathbf{x}}{\rho} = (\cos\phi_b, \sin\phi_b) \cdot (\cos\phi, \sin\phi) = \cos(\phi - \phi_b).$$

In case 3, we begin by noting that

$$\mathbf{v}^\varepsilon_{\phi+} \cdot \frac{\mathbf{x}' - \mathbf{x}}{\rho} = \cos(\phi - \phi^\varepsilon_{\phi+}),$$

and we also need to express $\mathbf{v}^\varepsilon_{\phi+}$ in terms of $\mathbf{v}^\varepsilon_{\phi-} = (\cos\phi^\varepsilon_-, \sin\phi^\varepsilon_-)$ and its perpendicular vector $(\mathbf{v}^\varepsilon_{\phi-})^\perp = (-\sin\phi^\varepsilon_-, \cos\phi^\varepsilon_-)$; that is,

$$\mathbf{v}^\varepsilon_{\phi+} = (\mathbf{v}^\varepsilon_{\phi+} \cdot \mathbf{v}^\varepsilon_{\phi-})\mathbf{v}^\varepsilon_{\phi-} + [\mathbf{v}^\varepsilon_{\phi+} \cdot (\mathbf{v}^\varepsilon_{\phi-})^\perp](\mathbf{v}^\varepsilon_{\phi-})^\perp.$$

Also, we need

$$\mathbf{v}^\varepsilon_{\phi-} \cdot \frac{\mathbf{x}' - \mathbf{x}}{\rho} = \cos(\phi - \phi^\varepsilon_-)$$

and

$$(\mathbf{v}^\varepsilon_{\phi-})^\perp \cdot \frac{\mathbf{x}' - \mathbf{x}}{\rho} = \sin(\phi - \phi^\varepsilon_-),$$

so that it is easy to verify that

$$(\mathbf{v}^\varepsilon_{\phi+} \cdot \mathbf{v}^\varepsilon_{\phi-}) = \cos(\phi^\varepsilon_+ - \phi^\varepsilon_-) = -\cos(\mu_\varepsilon(\delta(\mathbf{x}))\pi).$$

We use the decomposition of $\mathbf{v}^{\varepsilon}_{\phi+}$ on the basis given by $\mathbf{v}^{\varepsilon}_{\phi-}$ and $(\mathbf{v}^{\varepsilon}_{\phi-})^{\perp}$. In particular, we need

$$(\mathbf{v}^{\varepsilon}_{\phi+})^{\perp} \cdot \frac{\mathbf{x}' - \mathbf{x}}{\rho} = \sin(\phi - \phi^{\varepsilon}_{+})$$

and

$$(\mathbf{v}^{\varepsilon}_{\phi+})^{\perp} \cdot (\mathbf{v}^{\varepsilon}_{\phi-}) = \sin(\phi^{\varepsilon}_{-} - \phi^{\varepsilon}_{+}) = \sin(\mu_{\varepsilon}(\delta(\mathbf{x}))\pi).$$

Using the above formulas and following the approach in Moorcroft and Lewis (2006), we obtain

$$c^{\varepsilon} \cdot \mathbf{v}_b = \lim_{\tau \to 0} \frac{\bar{\rho}_{\tau}}{\tau} \frac{I_1(\kappa_{\tau})}{I_0(\kappa_{\tau})},$$

$$c^{\varepsilon} \cdot \mathbf{v}^{\varepsilon}_{\phi+} = \lim_{\tau \to 0} \frac{\bar{\rho}_{\tau}}{\tau} [\psi - (1 - \psi)\cos(\mu_{\varepsilon}(\delta(\mathbf{x}))\pi)] \frac{I_1(\kappa)}{I_0(\kappa)},$$

and

$$c^{\varepsilon} \cdot (\mathbf{v}^{\varepsilon}_{\phi+})^{\perp} = \lim_{\tau \to 0} \frac{\bar{\rho}_{\tau}}{\tau} (1 - \psi)\sin(\mu_{\varepsilon}(\delta(\mathbf{x}))\pi) \frac{I_1(\kappa)}{I_0(\kappa)}.$$

By taking the Taylor approximations of I_1 and I_0 and retaining only the lowest-order terms, we obtain

$$\frac{I_1(\kappa_{\tau})}{I_0(\kappa_{\tau})} \approx \frac{1}{2}\kappa_{\tau}.$$

We use this approximation and the assumptions for $\bar{\rho}$ and κ_{τ} to estimate values for c^{ε}: $c^{\varepsilon} \cdot \mathbf{v}_b \approx b(\rho_0^2/2)$ and

$$c^{\varepsilon} \cdot \mathbf{v}^{\varepsilon}_{\phi+} \approx b\frac{\rho_0^2}{2}[\psi - (1 - \psi)\cos(\mu_{\varepsilon}(\delta(\mathbf{x}))\pi)],$$

$$c^{\varepsilon} \cdot (\mathbf{v}^{\varepsilon}_{\phi+})^{\perp} \approx b\frac{\rho_0^2}{2}(1 - \psi)\sin(\mu_{\varepsilon}(\delta(\mathbf{x}))\pi).$$

The values of the diffusion coefficients are obtained exactly as described in Moorcroft and Lewis (2006), and we refer the reader to that work for the details. We have

$$d_{xx} = d_{yy} \approx \frac{\rho_0^2}{2}$$

and

$$d_{xy} = d_{yx} = 0.$$

Numerical Solutions: Finite Element Method

The partial differential equation (1) is solved using a finite element method approximation. The PDE (eq. [A2]) is first written under the form

$$\frac{\partial u(\mathbf{x}, t)}{\partial t} - \nabla \cdot (d(\mathbf{x})\nabla u) - (\nabla \cdot c(\mathbf{x}))u - (c(\mathbf{x}) \cdot \nabla u) = 0.$$

Multiplying all terms by a test function $\tilde{w}$ and integrating over the domain Ω, we get

$$\int_{\Omega} \left[\frac{\partial u(\mathbf{x}, t)}{\partial t} \tilde{w} - \nabla \cdot (d(\mathbf{x})\nabla u)\tilde{w} - (\nabla \cdot c(\mathbf{x}))u\tilde{w} - (c(\mathbf{x}) \cdot \nabla u)\tilde{w} \right] dx = 0,$$

where the second and last terms on the left-hand side are, respectively, the diffusion and advection terms. Classical Galerkin variational formulations are unstable for advection-diffusion equations, and consequently, a Streamline-Upwind

Petrov-Galerkin formulation proposed by Hughes and Brooks (1982) was used. This imposes a particular form for the test function $\tilde{w}$, and we refer readers to Hughes and Brooks (1982) for the details. Integrating by parts, the second term is

$$\int_{\Omega}\left[\frac{\partial u(\mathbf{x}, t)}{\partial t}\tilde{w} + (d(\mathbf{x})\nabla u)\cdot\nabla\tilde{w} - (\nabla\cdot c(\mathbf{x}))u\tilde{w} - (c(\mathbf{x})\cdot\nabla u)\tilde{w}\right]dx - \int_{\partial\Omega}(d(\mathbf{x})\nabla u\cdot\mathbf{N})\tilde{w}ds = 0.$$

Imposing the boundary condition (eq. [A3]) is equivalent to

$$\int_{\Omega}\left[\frac{\partial u(\mathbf{x}, t)}{\partial t}\tilde{w} + (d(\mathbf{x})\nabla u)\cdot\nabla\tilde{w} - (\nabla\cdot c(\mathbf{x}))u\tilde{w} - (c(\mathbf{x})\cdot\nabla u)\tilde{w}\right]dx - \int_{\partial\Omega}(c(\mathbf{x})\cdot\mathbf{N})u\tilde{w}ds = 0.$$

The time derivative is discretized by a two-step backward implicit scheme:

$$\frac{\partial u(\mathbf{x}, t)}{\partial t} \simeq \frac{3u^n - 4u^{n-1} + u^{n-2}}{2\Delta t},$$

where u^n is the solution at time $n\Delta t$. The time step Δt was set to 0.0025 in the numerical simulations. Quadratic triangular elements (P_2; see Bathe 1996) were used for the discretization in space. The global numerical scheme is thus second-order accurate in both space and time. A mesh with 3,200 elements was used, resulting in linear systems with around 6,500 unknowns that must be solved at each time step.

Literature Cited Only in Appendix A

Bathe, K. J. 1996. Finite element procedures. Prentice Hall, Englewood Cliffs, NJ.

Hughes, T. J. R., and A. Brooks. 1982. A theoretical framework for Petrov-Galerkin methods with discontinuous weighting functions: application to the streamline-upwind procedure. Pages 47–65 *in* R. H. Gallagher, D. H. Norrie, J. T. Oden, and O. C. Zienkiewicz, eds. Finite elements in fluid. Vol. 4. Wiley, London.

 DOI: 10.1086/670243

Appendix B from D. Fortin et al., "Movement Responses of Caribou to Human-Induced Habitat Edges Lead to Their Aggregation near Anthropogenic Features"

(Am. Nat., vol. 181, no. 6, p. 827)

Additional Figures

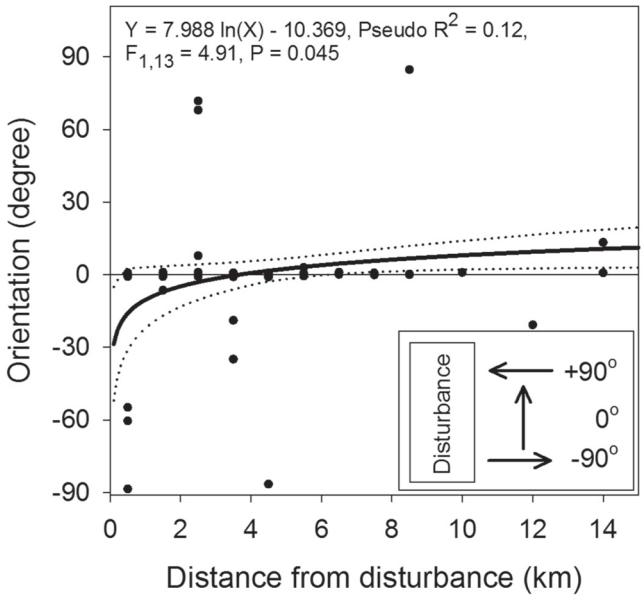

Figure B1: Change in mean orientation (with 95% confidence interval) with respect to the nearest road or cut as a function of distance from these anthropogenic features for caribou during intercamp movements. For example, caribou traveling perpendicularly away from the nearest disturbed area were assigned $-90°$, as depicted in the inset at the bottom right. From this relationship, ε corresponds to 3.7 km (i.e., the x-intercept). The pseudo-R^2 statistic was estimated as the square of the Pearson correlation statistic between predicted and observed values.

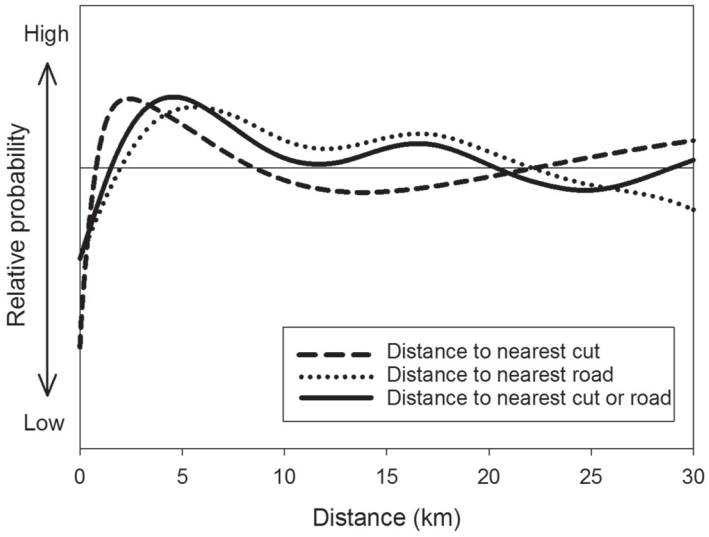

Figure B2: Relative probability of caribou occurrence in winter as a function of the distance to the nearest clear-cut, to the nearest road, or to either, as predicted from a semiparametric generalized additive model with a binomial distribution that contrasted locations with and without a track network. In all cases, the relative probability first increases sharply and then declines before oscillating at an intermediate level.